Synthesis and catalytic activity of manganese dioxide (type OMS-2) for the abatement of oxygenated VOCs

M. Andrés Peluso [a], Luis A. Gambaro [a], Estela Pronsato [b], Delia Gazzoli [c], Horacio J. Thomas [a], Jorge E. Sambeth [a,*]

[a] Centro de Investigación y Desarrollo en Ciencias Aplicadas, "Dr. Jorge J. Ronco" (FCE UNLP, CONICET), 47 Nro. 257 (1900) La Plata, Argentina
[b] Universidad Nacional del Sur, Dpto. de Física Bahia Blanca, Argentina
[c] Istituto di Sistemi Complessi (ISC), CNR-Universitá La Sapienza di Roma, Roma, Italy

Abstract

Two solids were synthesized by the reaction between Mn^{2+} and $KMnO_4$ in different order. The results of the characterization of both solids showed that: (i) they are poorly crystalline, although both belong to the Cryptomelane (OMS-2) phase; (ii) these materials are mesoporous (mesopores concentration in the order of 80%); (iii) they contain the couple Mn^{3+}/Mn^{4+}, being the Mn^{3+} concentration a function of the preparation method. Both catalysts were analyzed in the total oxidation of ethanol and the percentage of ethanol conversion on both solids reached 50% at 155 °C. The adsorption studies of methanol and ethanol have demonstrated the presence of basic sites and two different adsorption sites. The analysis of the results suggest that the amount of adsorbed ethanol molecules and the lowest temperature of CO_2 desorption detected is due to the Mn^{3+} concentration. This phenomenon is ascribed to a high concentration of Mn^{3+} which could originate a weak Mn–O bond and the formation of more active oxygen species which would improve the catalytic performance.
© 2007 Elsevier B.V. All rights reserved.

Keywords: Cryptomelane; Manganese oxide; TPD-MS; VOCs elimination

1. Introduction

Various manganese oxides have been reported as catalytic materials in the oxidation of many pollutants such as of phenol, ethanol, ethyl acetate, benzene, CO and propene [1–10], such as β-MnO_2, Mn_2O_3, γ-MnO_2, α-MnO_2 and OMS-2. Gil et al. [11], Spinicci et al. [12], Peluso et al. [13] have demonstrated that manganese oxides are the most efficient solids for catalytic elimination of pollutants, and this ability is associated to the presence of Mn^{3+}–Mn^{4+} ions and the formation of OH groups.

The Cryptomelane structure, which chemical molecular formula can be written as $K_x Mn^{4+}_{8-x} Mn^{3+}_x O_{16}$ ($0.2 \leq x \leq 1$), belongs to the octahedral molecular sieves type 2 family (OMS-2). The OMS-2 are a form of MnO_2, which have a tunnel-structure with a size of 4.6×4.6. The presence of Mn^{3+} and Mn^{4+} and a long the open structure of the OMS-2, lead to interesting physicochemical properties such as a high capacity of adsorption and a high electrical conductivity, which is related with the catalytic performance [14–18]. The experimental methods to synthesize OMS-2 are: (i) the oxidation of Mn^{2+} by $KMnO_4$ [19]; (ii) the oxidation of Mn^{2+} by refluxing with permanganate [20]; (iii) hydrothermal reaction using birnessite [21]; and (iv) sol–gel route [22]. Recently, Ding et al. [23] have synthesized an OMS-2 via a low temperature solvent-free method. The main result, of these authors, is that the increase in the alcohol conversion is due to the surface properties, such as the high surface area and the presence of a mesoporous in a percentage near to 90%.

The aim of this work is: to correlate the crystalline structure and the oxidation states of Mn in the OMS-2 and to analyze the presence of acid and basic sites over the catalysts and the different adsorption sites in the ethanol oxidation, with its catalytic properties.

* Corresponding author.
E-mail address: sambeth@quimica.unlp.edu.ar (J.E. Sambeth).

2. Experimental

2.1. Catalysts

Two samples were synthesized through $Mn(NO_3)_2$ oxidation with $KMnO_4$. One of them was synthesized by reaction between 50 mL of $KMnO_4$ 0.8% (Anedra 99%) and 50 mL of $Mn(NO_3)_2$ 0.05 M (Per analysis), which was added drop to drop wisely. The sample was dried to 120 °C for 24 h. The solid was calcined in air at 350 °C for 2 h. The oxide is named hereinafter MK1-350.

The second solid was prepared by the addition drop to drop of $KMnO_4$ (50 mL 0.8%) on $Mn(NO_3)_2$ (50 mL, 0.05 M). The solids were dried at 120 °C and calcined at 350 (MK2-350).

The samples were calcined at 350 °C, because Peluso [13,24] has showed that a higher temperature (450 °C) Mn_2O_3 can be formed and the catalytic performance is a function of the presence of this phases.

Mn_2O_3 catalyst was prepared by oxidation of $MnCO_3$ at 700 °C in flow of air and β-MnO_2 is a commercial sample (Baker 99%).

2.2. Characterization

The BET surface areas, total pore volume and average pore diameter of the samples were determined using a Micromeritics ASAP 2000. The samples were characterized by X-ray diffraction methods using a Phillips Diffractometer. The diffraction patterns were recorded using Cu Kα (L = 1.5406 A) radiation at 2 °min^{-1} scanning speed. The diffraction patterns were taken at room temperature in the $5 < 2\theta < 70°$ range. The XPS spectra were sequentially acquired by a computer using a Leybold Heraeus LHS10 spectrometer, operating in FAT mode, with Al (1486.6 eV) and Mg (1253.6 eV) radiation at a pressure lower than 10^{-8} Torr. The samples were manually pressed onto a platinum plate attached to the sample rod. Binding energy (BE) values were referenced to C1s at 285.0 eV and measured with an accuracy of ±0.2 eV.

2.3. Catalytic performance

Ethanol was chosen as a probe molecule because it is an important VOC's produced in the fermentation and sponge dough processes and the industrial production of beer, food or pharmaceutical products [25]. Catalytic test was carried out at atmospheric pressure in a continuous flow tubular glass reactor. Two hundred milligrams of the sample were loaded as a fine powder. The total gas flow of ethanol–air was 20 cm^3 min^{-1} and the reaction temperatures were in the range 100–300 °C. The feed composition was 900 ppm of ethanol in air, with an excess of O_2.

2.4. Kinetic of ethanol adsorption

The ethanol adsorption was analyzed as a function of time with the aim of determining: (i) the quantity of ethanol molecules adsorbed and (ii) the number of sites where the ethanol molecules could be adsorbed. Kinetic studies were carried out in volumetric equipment according to the description by Quaranta et al. [26]. Ethanol pressure was measured with MKS capacitance manometer 310 BHS. The samples were pre-treated at 100 °C and 1.3×10^{-4} Pa in a flow of O_2 for 3 h in order to stabilize the catalyst surface. After pre-treatment, the reactor temperature was brought to the adsorption temperature (50 °C) and the system was allowed to reach the equilibrium pressure. An initial ethanol pulse of 30 Pa was admitted to the reactor and when the system reached the new equilibrium pressure, a second ethanol pulse of 30 Pa was added. The adsorption rate was measured continuously by recording pressure changes of the system while the gas was adsorbed on the catalyst. In this way, when the kinetic measurement was finished the pressure of the system was still higher than that necessary to reach maximum coverage at each temperature.

2.5. Temperature programmed desorption mass spectrometry (TPD-MS)

TPD-MS study was made using a Balzer QSM 112A. The sample (100 mg) was placed in a quartz reactor and pre-treated in O_2 (35 ml min^{-1}) at 300 °C for 1 h. After pre-treatment, the sample was cooled to 50 °C under a flow of He. Successive pulses of 0.5 μL of alcohol were dosed through a heated septum until the saturation of the catalysts is reached. In this work two alcohols were used (i) methanol, to characterize the nature of the active sites of catalysts [27] and (ii) ethanol, to analyze the reaction pathway according to the ethanol desorption and the formation of CO_2 and H_2O. The system is heated up to 350 °C at 10 °C min^{-1} after the saturation of the catalyst.

3. Results and discussion

The XRD spectra of the prepared materials are presented in Fig. 1. The XRD patterns show a poorly ordered manganese oxide phase. In both MK1-350 and MK2-350 catalysts the
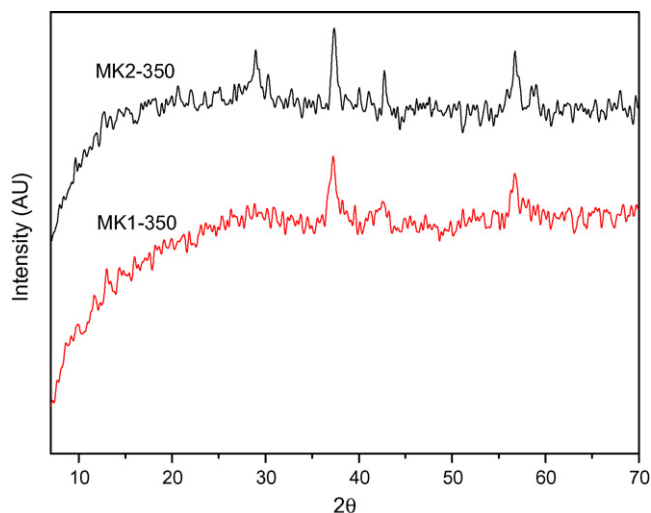

Fig. 1. X-ray powder diffraction patterns of the MK samples.

Table 1
BET surface areas, crystalline size the MK samples and BET surface areas of β-MnO_2 and Mn_2O_3

Sample	BET surface area ($m^2 g^{-1}$)	Crystallite size (nm)	Total pore volume (cm^3/g)	Average pore diameter (nm)
β-MnO_2	5.6			
Mn_2O_3	11.6			
MK1-350	82.3	15	0.347	9.5
MK2-350	68.3	27	0.293	16.9

peaks at $37.2°$ (2 1 1), $42.7°$ (3 0 1) and $56.4°$ (6 0 0) are detected and only in the MK2-350 sample one signal at $28.6°$ is observed. The results of the surface area, crystalline size, total pore volume and average pore diameter are summarized in Table 1. As it can be seen, the MK1-350 average pore size is smaller than the MK2-350 catalyst; this result explains why the MK1-350 surface area is higher than the MK2-350 sample. With respect to the total pore volume the same behaviour is observed. According to Post and Burnham [28], these results might be ascribed to the effect in the parameters of unit cell originated by the Mn^{3+} distortions, which is of the order of 0.04 nm. So, a considerable amount of Mn^{3+} ions can generate a large distortion. In this sense, as it can be seen in Table 2, the Mn^{3+} concentration in MK1-350 sample is larger than in MK2-350 catalysts, therefore a larger distortion is expected.

In both catalysts, the distribution percentage of pore sizes was similar; in the MK1-350 sample: (i) micropores 5.2%; (ii) mesopores 80.0%; and (iii) macropores 14.8% and in the MK2-350: (i) micropores 5.3%; (ii) mesopores 75.7%; and (iii) macropores 19.0%. These results showed that the amount of macropores formed in the MK catalysts are lower than the OMS-2 catalysts prepared by traditional methods, whose values are in the order of 55%. In this sense, Ding et al. [23] have recently demonstrated that the method of preparation of cryptomelane has great influence over the morphology, structural properties and catalytic activity. They showed that a high surface area, a high mesopore concentrations and a small particle size improve the catalytic performance.

The manganese spectroscopic features of manganese oxides have been widely reported and discussed in the literature [17,29–31]. The Mn2p region, characterized by a spin-orbit splitting ($2p_{3/2}$–$2p_{1/2}$) of 11.4–11.6 eV, is broadened by multiplet splitting and satellite structures. MnO has shake-up peaks at about 5 eV from both the 2p peaks, Mn_2O_3 and MnO_2 clearly show the satellite associated with the $2p_{1/2}$ main peak, while that associated to the $2p_{3/2}$ overlaps with the $2p_{1/2}$ main component. Compounds having no unpaired electrons, such as $KMnO_4$, give symmetrical peak with no shake up features. The Mn3s level shows a multiplet splitting which varies with the chemical state: the higher the oxidation state, the lower the splitting [17,24,31]. Although a general agreement exists in the literature about the binding energy values (BE) associated to different chemical state the identification of the different surface species is rather complex because of the small BE shift between the different oxidation states and the usual broadness of the peaks. The XPS results are presented in Table 2.

For all the samples the O1s peak is in general composed by three components at about $529.8 ± 0.2$ eV, $531.4 ± 0.4$ eV and 533.2 eV $± 0.6$ eV, attributed to O^{2-}, OH groups and adsorbed molecular water.

Distinct Mn2p features were recorded on the various compounds. β-MnO_2 was characterized by a rather narrow Mn2p region features with $Mn2p_{3/2}$ at 642.9 eV (2.8 eV), due to Mn(IV), in agreement with literature data. The Mn3s components show a splitting of 4.4 eV. The Mn 2p region of Mn_2O_3 was decomposed by one component with $Mn2p_{3/2}$ peaks at 641.3 eV (2.8 eV) assigned to Mn(III). The Mn 3s multiplet splitting was 5.7 eV, in agreement with the values for Mn(III). Similar features were detected for the MK1-350 and MK2-350 samples. The Mn2p spectral shape could be reproduced with a $Mn2p_{3/2}$ components at 641.8 eV (2.5 eV) and at 641.4 eV (2.3 eV) ascribed to Mn(III), and at 643.2 eV

Table 2
Binding Energy (eV) of Mn2p and O1s

Sample	Mn $2p_{3/2}$ (eV)	Mn$2p_{3/2}$ (eV)	% Mn	O 1s (eV)	% O	ΔE Mn 3s (eV)	AOS
MnO_2	642.9 (2.6)	642.7 (2.6)	Mn^{4+}	529.8 (1.4)	40 O^{2-}	4.4	4
		644.4		531.1 (2.8)	38 OH^-		
				533.8 (3.0)	22 H_2O		
Mn_2O_3	642.3 (3.8)	641.3 (2.8)	Mn^{3+}	530.1 (1.8)	40 O^{2-}	5.7	3
		645.6					
MK1-350	642.7 (3.5)	641.8 (2.5)	52 Mn^{3+}	529.8 (1.5)	64 O^{2-}	5	3.6
		643.2 (2.4)	48 Mn^{4+}	531.2 (2.2)	28 OH^-		
		645.3		533.0 (2.6)	8 H_2O		
MK2-350	642.6 (3.5)	641.4 (2.3)	30 Mn^{3+}	529.7 (1.6)	66 O^{2-}	5	3.8
		642.7 (2.8)	70 Mn^{4+}	531.3 (2.1)	28 OH^-		
		645.1		533.0 (1.6)	6 H_2O		

Compositions of Mn and O and splitting width of Mn3s (eV) and AOS: average oxidation state of Mn.

(2.4 eV) and 642.7 eV (2.8 eV) attributed to Mn(IV). According with Nesbitt and Banerjee [32] the Binding Energy of 644.1 eV detected in β-MnO$_2$ and the component at 645 eV detected in both MK catalysts could be assigned to Mn^{4+} free and Mn^{3+} bonded to O^{2-} and/or OH$^-$, respectively.

According to the literature, to determine the surface chemical states one may use the Mn2p and the associated satellites BE values, the Mn2p$_{3/2}$-O1s separation, the Mn3s multiplet splitting or peak synthesis procedures [17]. The correlation between the Binding Energy (Mn2p$_{3/2}$-O1s) and Mn3s multiplet splitting allow us to say that the average oxidation states (AOS) of the MK samples are between 3.6 and 3.8, which are in agreement with the results of Cai et al. [33] and Barrio et al. [17], who have reported AOS between 3.5 and 3.8.

Different authors [33,34] have showed that OMS-2 possess basic sites. On the basis of the conclusions reported by Briand [27], who have analyzed the methanol oxidation over oxides, the formation of H$_2$CO is produced on REDOX sites and the formation of (CH$_3$)$_2$O and CO$_2$ over acid and basic sites respectively. The results of the CH$_3$OH adsorption–oxidation can be observed in the Fig. 2a and b. The TPD-MS analysis

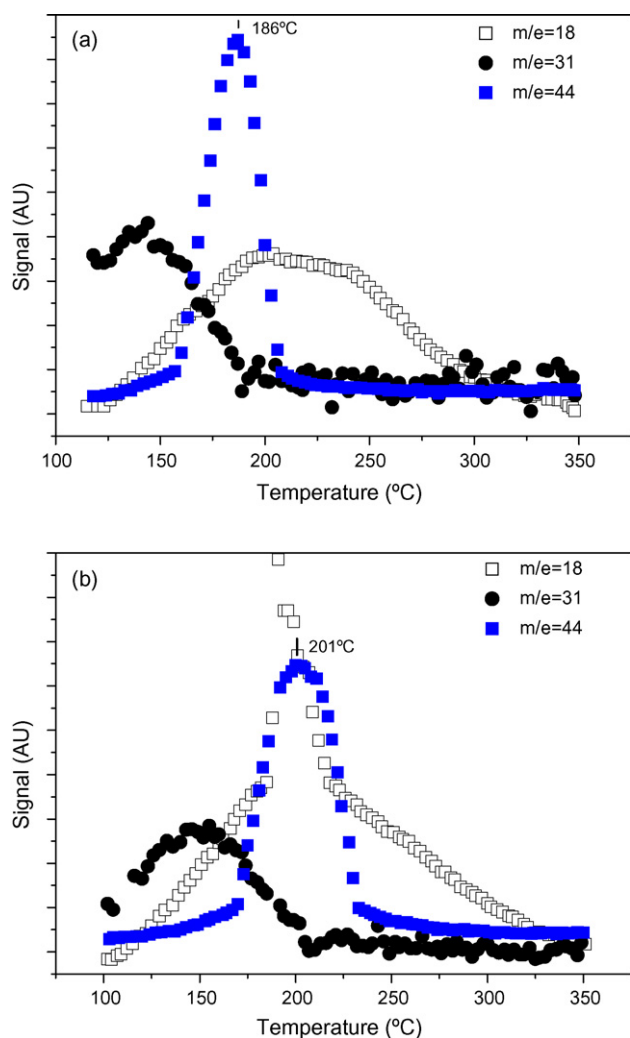allows us to see that one peak of methanol (m/e = 31) is detected in both catalysts between 140 and 150 °C. The formation of H$_2$CO (formaldehyde, m/e = 29) and (CH$_3$)$_2$O are not observed, although over MK1-350 catalyst at 186 °C and over MK2-350 catalyst at 201 °C, CO$_2$ (m/e = 44) is desorbed. In the first place, these results suggest that there are no REDOX and acidic sites in the catalysts prepared. These results are coincident with the reports of Cai et al. [33], who have shown by NH$_3$ and CO$_2$ adsorption, that the cryptomelanes have basic sites. In the second place, CO$_2$ is desorbed at lower temperature in MK1-350 catalyst than in MK2-350, which could be associated to the Mn^{3+}/Mn^{4+} ratio. A high concentration of Mn^{3+} instead of Mn^{4+} could originate a weak Mn–O bond, and this phenomenon may lead to the formation of more active oxygen species in the lattice which would improve the methanol dissociation by subtracting H from the methanol molecule.

The characterization results showed that: (i) both MK materials belong to the cryptomelane phase; (ii) Mn^{3+} concentration is higher in the MK1-350 catalyst than in the MK2-350 sample; (iii) the surface area and total pore volume are larger in the MK1-350 than in the MK2-350; and (iv) on both catalysts the CH$_3$OH adsorption demonstrated the presence of basic sites.

Fig. 3 shows the catalytic activity measurements of ethanol oxidation. We can observe the ethanol conversion for both MK, together with the results of the βMnO$_2$ and Mn$_2$O$_3$ catalysts. The percentage of ethanol conversion on MK catalysts reached 50% at 155 °C (T$_{50}$), whereas the other solids have a T$_{50}$ at T > 200 °C (Fig. 3). βMnO$_2$ and Mn$_2$O$_3$ belong to the pyrolusite and bixbyite phases respectively, whose oxidation numbers are 4+ and 3+. Mn$_2$O$_3$ and βMnO$_2$ have a defined crystalline structure and are stoichiometric solids, which could originate a pronounced decrease in catalytic activity, according to Stobbe et al. [35] and Shaheen and Selim [36]. Both characterization and catalytic conversion results indicate that the high activity of MK synthesized are due to the Mn^{3+}–Mn^{4+} couple, the tunnel structure and the presence of basic sites.

Fig. 2. TPD-MS spectra of CH$_3$OH onto (a) MK1-350 and (b) MK2-350. (Reference m/e = 18 H$_2$O; m/e = 31 CH$_3$OH; m/e = 44 CO$_2$).
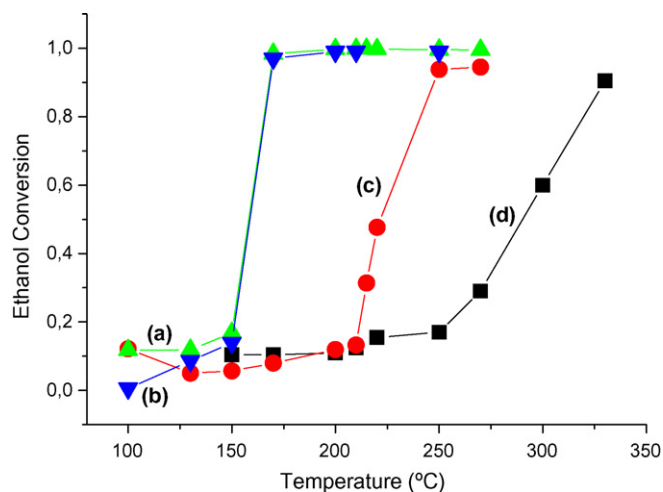

Fig. 3. Ethanol conversion: (a) MK1-350; (b) MK2-350; (c) Mn$_2$O$_3$; (d) βMnO$_2$.

Kinetics measurements of ethanol chemisorption on both MK samples were performed at 50 °C. The data was analyzed by Langmuir and Elovich equations [26] and the best fit was obtained with Elovich model. The results were tested by using the integrated form, where the amount of adsorbed molecules is plotted as a function of the natural logarithm of the adsorption time. Fig. 4a and b shows the experimental data, which showed two different behaviours. These results can be explained on the basis of adsorbate–absorbent interaction and superficial heterogeneities. According to Elovich's model, this behaviour indicates that there are two different adsorption sites, which can be either energetically or structurally different.

Considering these results, the ethanol adsorption on MK was analyzed by TPD-MS in a flow of helium. The Fig. 5a and b show that both catalysts have two peaks of CO_2 desorption. In this case, the results are comparable with CH_3OH adsorption, CO_2 desorbed at lower temperature in MK1-350 sample than in MK2-350. On the other hand, two desorption peaks are detected which indicate the presence of two different adsorption sites on both MK catalysts, which could be O^{-2} and OH^- according to the XPS results.

In summary, both solids are mesoporous and the average oxidation states are between 3.6 and 3.8. The catalysts posses an excellent activity in the total oxidation of ethanol which is related to: the presence of the couple Mn^{3+}–Mn^{4+}, the tunnel structure and basic sites. On the other hand, the studies by TPD-
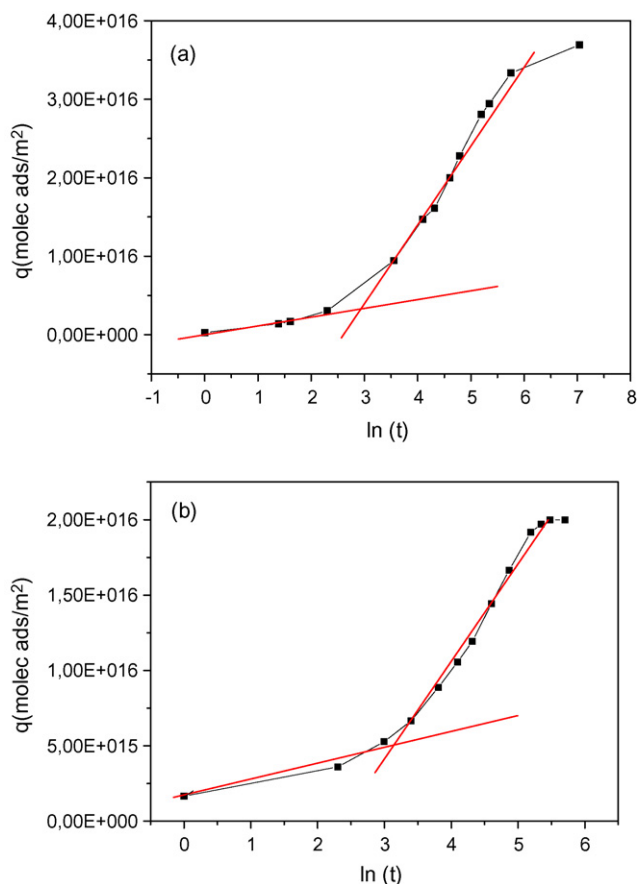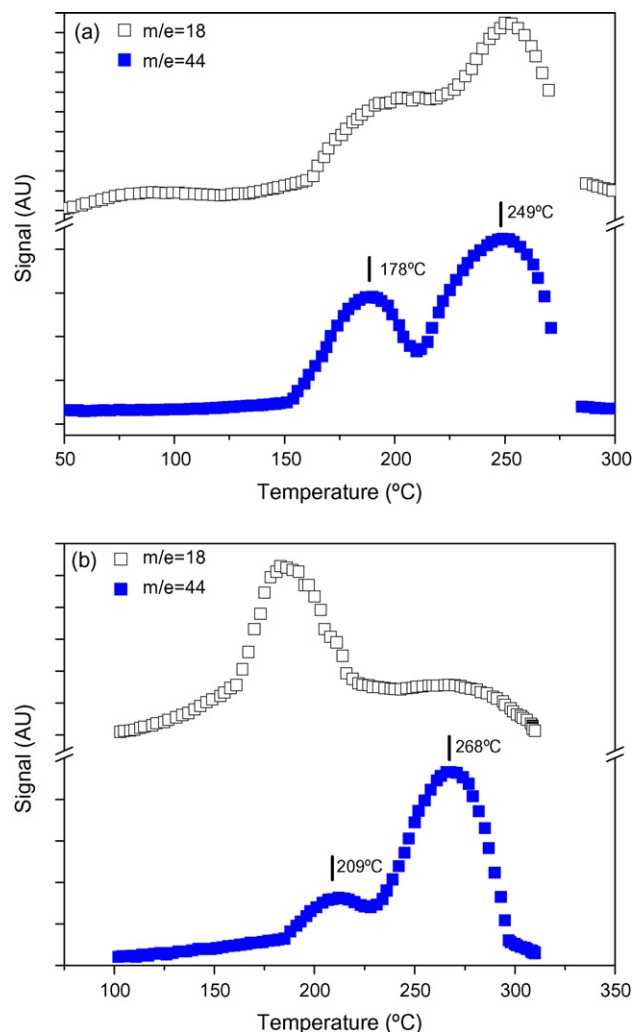
Fig. 5. TPD-MS spectra of CH_3CH_2OH onto (a) MK1-350 and (b) MK2-350 (reference Fig. 2).

MS and the ethanol adsorption kinetics have shown the presence of two different sites of adsorption-reaction. Finally, in the MK1-350 catalyst, the amount of adsorbed ethanol molecules and the lowest temperature of CO_2 desorption detected could be due to the Mn^{3+} concentration, which is higher on this solid. A high concentration of Mn^{3+} could originate a weak Mn–O bond and the formation of oxygen species more active in the lattice which would improve the H subtraction from the adsorbed alcohol molecule.

4. Conclusions

Two solids were synthesized by chemical reaction between $Mn(NO_3)_2$ and $KMnO_4$ in different order and they were calcined at 350 °C. The characterization results showed: (i) the solids belonged to the cryptomelane (OMS-2) phase; (ii) the mesoporous concentration is in the order of 80% and (iii) the existence of the couple Mn^{3+}/Mn^{4+}, although the Mn^{3+} concentration is function of the preparation method. In this sense, when $Mn(NO_3)_2$ was added drop to drop on $KMnO_4$, the Mn^{3+} concentration increased.

Fig. 4. Elovich's plot for chemisorption of ethanol onto (a) MK1-350 and (b) MK2-350.

The catalysts were analyzed in the total oxidation of ethanol and the percentage ethanol conversion on both solids reached 50% at 155 °C and they were more active than Mn_2O_3 and βMnO_2.

The methanol and ethanol chemisorption has demonstrated the presence of basic sites and two different adsorption sites, respectively. These results, in a sense, allow us to say that the amount of adsorbed ethanol molecules and the lowest temperature of CO_2 desorption detected is due to the Mn^{3+} concentration, which is higher on MK1-350 catalyst. A high concentration of Mn^{3+} could originate a weak Mn–O bond and the formation of oxygen species more actives in the lattice which would improve the catalytic activity.

References

[1] S. Kanungo, K. Parida, B. Sant, Electrochim. Acta 26 (1981) 1147.
[2] R. Jothiramalingam, B. Viswanathan, T. Varadarajan, Catal. Commun. 6 (2005) 41.
[3] I.M. Goldman, J. Org. Chem. 34 (1969) 1979.
[4] V. Krishnan, S. Suib, J. Catal. 184 (1999) 305.
[5] T. Katranas, A. Godelitsas, A. Vlessidis, N. Evmiridis, Micropor. Mesopor. Mater. 69 (2004) 165.
[6] V. Makwana, L. Garces, L. Lui, J. Cai, Y. Son, S. Suib, Catal. Today 85 (2003) 225.
[7] L.E. Cadus, O. Ferretti, Appl. Catal. A 233 (2002) 239.
[8] R. Cracium, N. Dulamita, Ind. Eng. Chem. Res. 38 (1999) 1357.
[9] X. Run, X. Wang, D. Wang, K. Zhov, Y. Li, J. Catal. 237 (2006) 426.
[10] M. Paulis, L. Gandia, A. Gil, J. Sambeth, J. Odriozola, M. Montes, Appl. Catal. B 26 (2000) 37.
[11] A. Gil, L. Gandía, S. Korili, Appl. Catal. A 274 (2004) 229.
[12] R. Spinicci, M. Faticani, P. Marini, S. De Rossi, P. Porta, J. Mol. Catal. A 197 (2003) 147.
[13] M. Peluso, J. Sambeth, H. Thomas, React. Kinet. Catal. Lett. 80 (2003) 241.
[14] Y. Shen, S. Suib, C. Óyoung, J. Am. Chem. Soc. 116 (1994) 11020.
[15] S. Brock, S. Duan, Z. Tian, O. Giraldo, H. Zhour, S. Suib, Chem. Mater. 10 (1998) 2619.
[16] M. Abecassis-Wolfovich, R. Jothiramalingam, M. Landau, H. Herkowitz, B. Viswanathan, T. Varadarajan, Appl. Catal. B 59 (2005) 93.
[17] I. Barrio, I. Legórburu, M. Montes, M. Domínguez, M. Centeno, J. Odriozola, Catal. Lett. 101 (3/4) (2005) 151.
[18] F. Wolkeishtein, The Electronic Theory of Catalysis on Semiconductors, Pergamon Press, New York, USA, 1963.
[19] M. Cheney, N. Birkner, L. Ma, Th. Hartmann, P. Bhowmik, V. Hodge, S. Steinberg, Colloid Surf. A 289 (2006) 185.
[20] R. Jothiramalingam, B. Viswanathan, T. Varadarajan, Mater. Chem. Phys. 100 (2006) 257.
[21] X. Chen, Y. Shen, S. Suib, C. O'Young, Chem. Mater. 14 (2002) 940.
[22] S. Ching, E. Welch, S. Hughes, A. Bahadoor, S. Suib, Chem. Mater. 14 (2002) 1292.
[23] Y. Ding, X. Shen, S. Sithambaram, S. Gomez, R. Kumar, V. Crisostomo, S. Suib, M. Aindow, Chem. Mater. 17 (2005) 5382.
[24] M. Peluso, Doctoral Thesis, La Plata University, Argentine, 2006.
[25] A. Buonicore, in: Davids (Ed.), Air Pollution Engineering Manual, Air and Waste Management Association, 1992.
[26] N. Quaranta, L. Gambaro, H. Thomas, J. Catal. 107 (1987) 503.
[27] L. Briand, Investigation of the Nature and Number of Surface Active Sites of Supported and Bulk Metal Oxide Catalysts Through Methanol Chemisorption in "Metal Oxides: Chemistry and Applications", Ed. CRC Press Taylor & Francis, Florida, USA, 2005.
[28] J. Post, C. Burnham, Am. Miner. 71 (1986) 1178.
[29] S. Ponce, M. Peña, J. Fierro, Appl. Catal. B 24 (2000) 193.
[30] V. Di Castro, G. Polzonetti, J. Electron Spectrosc. Relat. Phenom. 48 (1989) 117.
[31] M. Toupin, T. Brousse, D. Belanger, Chem. Mater. 14 (2002) 3946.
[32] H. Nebitt, D. Banerjee, Am. Miner. 83 (1998) 305.
[33] J. Cai, J. Lui, W. Willis, S. Suib, Chem. Mater. 13 (2001) 2413.
[34] G. Xia, W. Tong, E. Tolentino, N. Duan, S. Brock, J. Wang, S. Suib, Chem. Mater. 13 (2001) 1585.
[35] E. Stobbe, B. de Boer, J. Geus, Catal. Today 47 (1999) 161.
[36] W. Shaheen, M. Selim, Thermochim. Acta 332 (1998) 117.